ELSEVIER

Journal of Nuclear Materials 276 (2000) 50–58

journal of nuclear materials

www.elsevier.nl/locate/jnucmat

The search for interstitial dislocation loops produced in displacement cascades at 20 K in copper

M.A. Kirk[a,*], M.L. Jenkins[b], H. Fukushima[c]

[a] *Materials Science Division, Argonne National Laboratory, Argonne, IL 60439, USA*
[b] *Department of Materials, University of Oxford, Parks Rd., Oxford OX1 3PH, UK*
[c] *Faculty of Engineering, Hiroshima University, Higashi-Hiroshima 739-8527, Japan*

Abstract

A low-temperature in situ ion-irradiation and annealing experiment has been performed in copper. Most clusters which persisted through an anneal to 120 K showed no size changes within the resolution (0.5 nm) of a new weak-beam sizing technique. Of the 55 defects measured under a range of weakly diffracting conditions, seven showed measurable size decreases while three showed size increases. We argue that these clusters are likely to be of vacancy and interstitial nature, respectively. Also on annealing to 120 K a fraction of about 25% of the clusters formed by irradiation with 600 kV Cu^+ ions at 20 K disappeared, while a similar number of clusters appeared at different locations. The remaining defects persisted through the anneal, sometimes however with modified morphologies. Video microscopy suggested that the disappearance and appearance of clusters occurred gradually and was unlikely to be due to loop movement. Some arguments on the possible nature of these clusters are presented. On warming specimens to room temperature, a high density of small stacking-fault tetrahedra appeared close to the electron-exit surface of the foil in regions which had been exposed to the electron beam at low temperatures. These are most likely due to the clustering of vacancies produced by sputtering at the back surface.

1. Introduction

The possible formation of interstitial dislocation loops in displacement cascades is a subject of considerable current interest to the radiation damage community. Molecular dynamics simulations suggest that appreciable interstitial clustering occurs in cascades (e.g. [1–3]), and some simulations have even predicted the production of loops large enough to be resolvable in the transmission electron microscope. There have also been reports of the identification of interstitial loops in experiments (e.g. [4,5]). However, our recent work on small point-defect clusters in copper produced by room-temperature heavy ion irradiation indicates that these experiments may be misleading. The conventional techniques for the identification of the nature of small clusters – the 2 1/2 D method, and the black–white contrast technique – both fail to identify the nature of a majority of the clusters. The 2 1/2 D method seems flawed in principle [6]. The black–white contrast technique works well for larger, first-layer, loops. These turned out to be exclusively vacancy in nature. However, it fails for smaller loops located closer to the foil center, which arguably are more likely to be interstitial [7]. It is therefore our view that valid and direct experimental evidence for the production of interstitial loops directly in cascade events has yet to be produced. In this paper, we exploit a recent improvement in facilities for low temperature in situ TEM and ion irradiations, and improvements in microscopy technique, to perform experiments in copper which seek evidence for these elusive defects.

2. Experimental details

The experiments described here were designed to investigate the nature of the defect clusters produced at low (20 K) irradiation temperature in copper by in situ

* Corresponding author. Tel.: +1-630 252 4998; fax: +1-630 252 4798.
E-mail address: kirk@anl.gov (M.A. Kirk)

0022-3115/00/$ - see front matter
PII: S0022-3115(99)00168-3

heavy-ion irradiation. An indirect technique was used to assess the interstitial or vacancy nature of a cluster defect. The principle was to measure the change in size of individual defects following an anneal through the free interstitial migration stage I, and subsequently a further anneal through the free vacancy migration stage III. Since only free interstitials are mobile in stage I, the shrinkage of a defect on annealing through this stage would imply its nature is vacancy. The same defect might be expected to grow on further annealing through stage III (although, as will be seen, experimental difficulties precluded explicit investigation of this). Interstitial clusters would be expected to show the opposite behavior.

In order to produce high energy collision cascades throughout the thickness of a typical TEM foil (ca. 60 nm), irradiations were performed with Cu^+ ions of energy 600 keV. Fig. 1 pictures typical examples. This energy was chosen on the basis of damage calculations using the modified [8] TRIM code [9], which shows that the damage energy distribution is very similar to that produced in a typical fission neutron spectrum (see Fig. 2). The distribution of damage energy gives the range of PKA recoil energies of importance to defect cascade events. The distribution of PKA recoils displays the higher fraction of low energy recoil events for the ion irradiation.

These calculated collision statistics illustrate a central idea behind the low temperature experiment. That is, to use this relatively high fraction of low energy collisions, which produces a concentration of point defects which become freely migrating upon annealing, to probe the nature (interstitial or vacancy) of the extended defects produced by the high energy recoil cascades. By sequentially annealing through stage 1 (interstitial migration) and stage 3 (vacancy migration), the size changes of the extended defects, dislocation loops or stacking fault tetrahedra, would thus indicate their natures. Producing the cascade defects throughout the foil thickness reduces the problem of a dominant surface

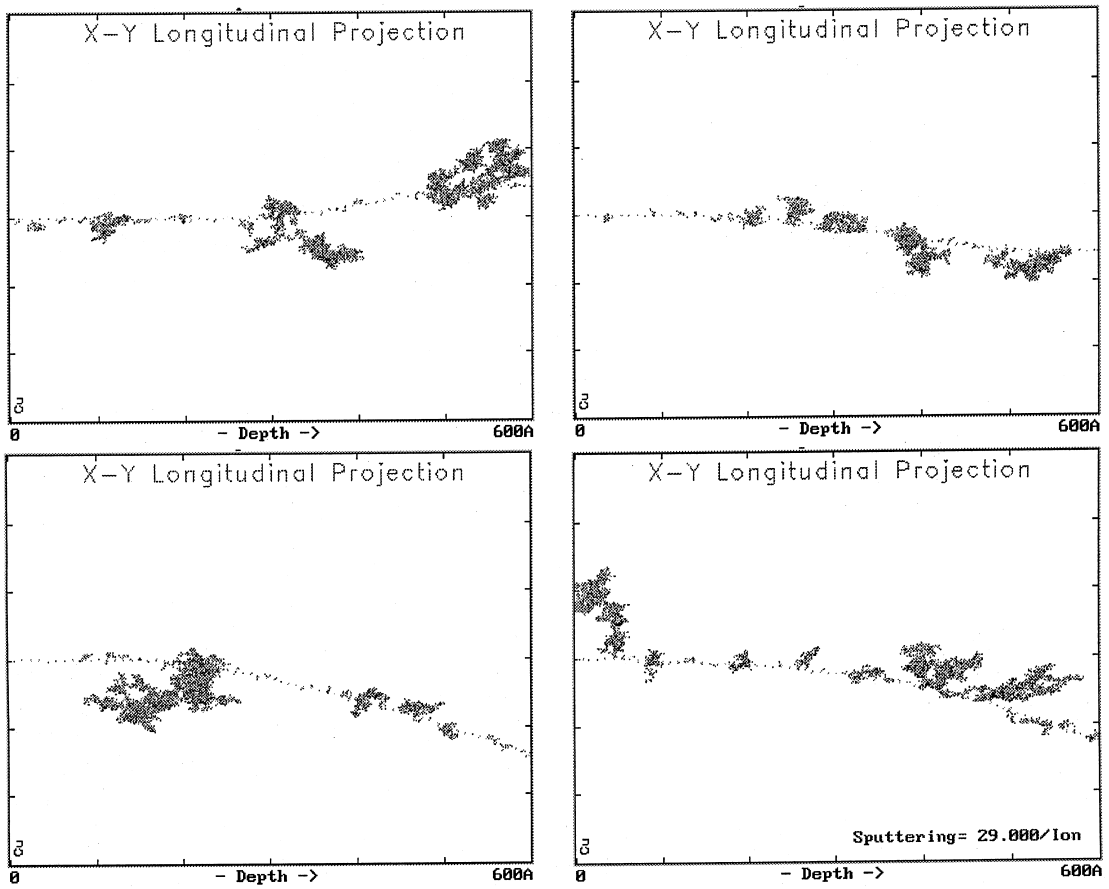

Fig. 1. Four examples of a single 600 keV Cu ion passage through a 60 nm Cu foil, as calculated by TRIM 96 [9]. Vacancies are represented as small black dots, while clusters of vacancies resulting from collision cascades produced by high energy recoils are clusters of black dots.

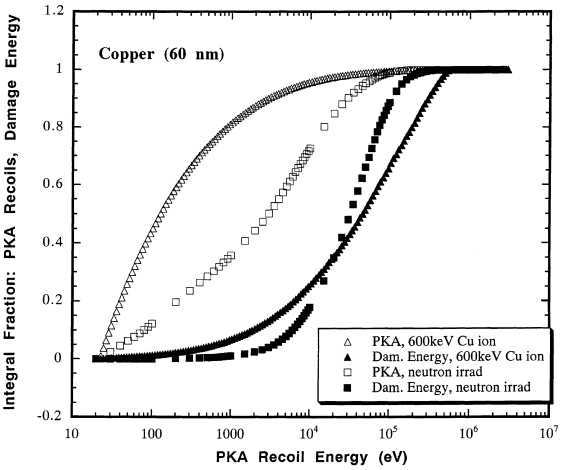

Fig. 2. Collision statistics comparing fission neutron and 600 keV Cu ion irradiations of 60 nm Cu, as calculated by a modified [8] version of TRIM 89 [9].

sink for migrating point defects, and any surface effects on cascade defect production itself.

Thin-foil specimens of pure single-crystal copper with orientations about 10° from (1 1 1) were prepared by electro-polishing 3 mm discs. They were immediately mounted into the sample holder of an Oxford Instruments low temperature stage, which was loaded into the Hitachi-9000 electron microscope of the Argonne Intermediate Voltage Electron Microscope Facility. The microscope was operated at 100 kV, for reasons given below. Regions chosen for microscopy were flat and of thickness about 50–60 nm, as estimated from {2 0 0} thickness contours (and subsequently confirmed by convergent-beam diffraction). The stage was cooled to 20 K and irradiations were performed in situ to a dose of 5×10^{14} ions m^{-2}, with the ion beam incident along a direction close to the foil normal. At this dose, individual ion impacts are on average well-separated, so that the probability of overlap of cascades produced by separate ions is quite small. Microscopy was performed using an operating reflection $g = 002$, with the foil oriented close to the [1 1 0] pole. This entailed tilting the specimen by about 23°. This had the advantage that the images of defect clusters, produced by the same ion in sub-cascades at different points along its track (Fig. 1), projected at closely spaced, but separate, positions. Most multiple defects produced by the same ion could therefore be identified separately.

Images were recorded after the initial irradiation at 20 K, and after both of the annealing steps, to 120 K and to room temperature. An improved weak-beam TEM technique, described in detail by Jenkins et al. [10] was used to measure the sizes of defects before and after the anneals. Following the recipe given in Ref. [10], we recorded a series of 5–7 weak-beam micrographs at each condition with a systematic variation of the deviation parameter from 0.2–0.3 nm^{-1}. All micrographs both before and after anneals were taken with the specimen cooled to 20 K to ensure that the image quality was uniform. The beam convergence semi-angle was held constant at about 0.25°. Size measurements were made from prints of total magnification 5×10^5 using a digitizing tablet. The prints of each micrograph were examined in random order. In each case, the maximum extent of each contrast figure was measured ten times, and averaged. Care was taken to measure each defect in the same direction in each micrograph. The direction was chosen based on defect geometry, when evident from the contrast shape. We then looked for systematic changes in the sizes of individual defects before and after annealing, checking for consistency across the full range of s values. We have shown that this procedure allows changes in the size of defects to be revealed and determined reliably, for defects located throughout a foil thickness of 60 nm, down to a resolution limit of about 0.5 nm. Finally, the specimens were transferred to a Philips CM30 microscope, the areas previously imaged were relocated, and foil thickness determinations were made with the standard convergent-beam method [11].

In a second experiment with the same irradiation conditions, a video recording was made during the warm-up from 20 to 120 K, with the specimen set in a (g, 4.5 g) weak-beam diffraction condition.

3. Results

Fig. 3 illustrates the changes in defects in the same area before and after a 15 min anneal at 120 K. Two of the seven values of s (in units of nm^{-1}) are shown as examples. The imaging diffraction vector $g = 002$, and the beam direction was about 13° from the 1 1 0 pole. The irradiation direction is arrowed, the length of the

Fig. 3. Examples of TEM micrographs of the same area taken after irradiation by 600 keV Cu ions to a dose of 5×10^{14} m^{-2} at a sample temperature of 20 K. The micrographs on the left were taken at 20 K immediately after irradiation. The micrographs on the right were taken at 20 K after the irradiation and a 15 min anneal to 120 K. All micrographs were taken in dark field under weakly diffracting conditions with $g = 002$, beam direction near the [1 1 0] pole, and examples of two of the seven weak beam conditions: $s = 0.24$ nm^{-1} (g, 5.25 g; top micrographs) or $s = 0.27$ nm^{-1} (g, 5.75 g; bottom micrographs) are illustrated. The irradiation direction is shown with an arrow whose length is equal to the projection of the ion path through this foil thickness of 55 nm. Labeled defects are discussed in the text.

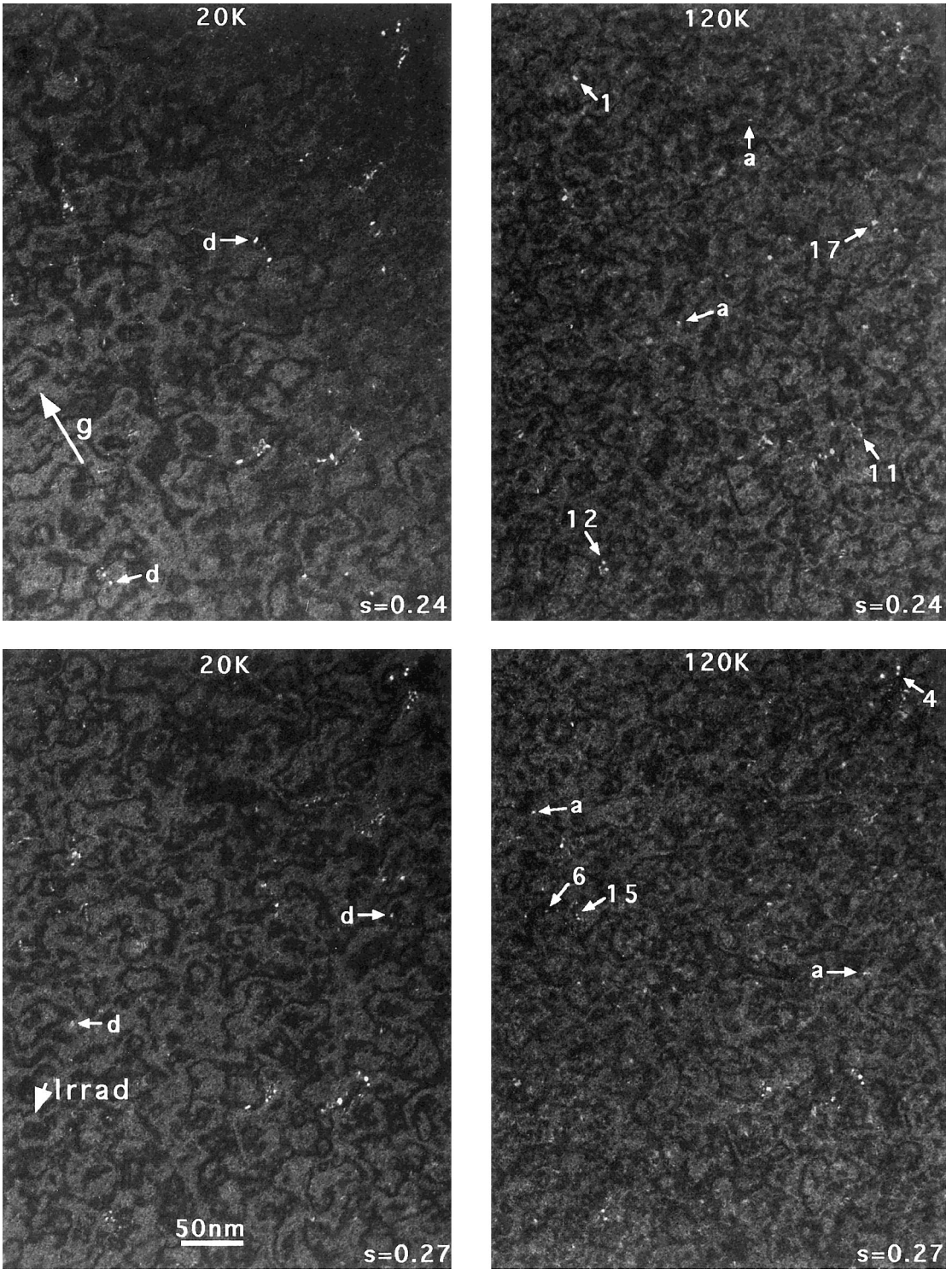
20K
d
g
d
s=0.24
120K
1
a
17
a
11
12
s=0.24
20K
d
d
Irrad
50nm
s=0.27
120K
4
a
6
15
a
s=0.27

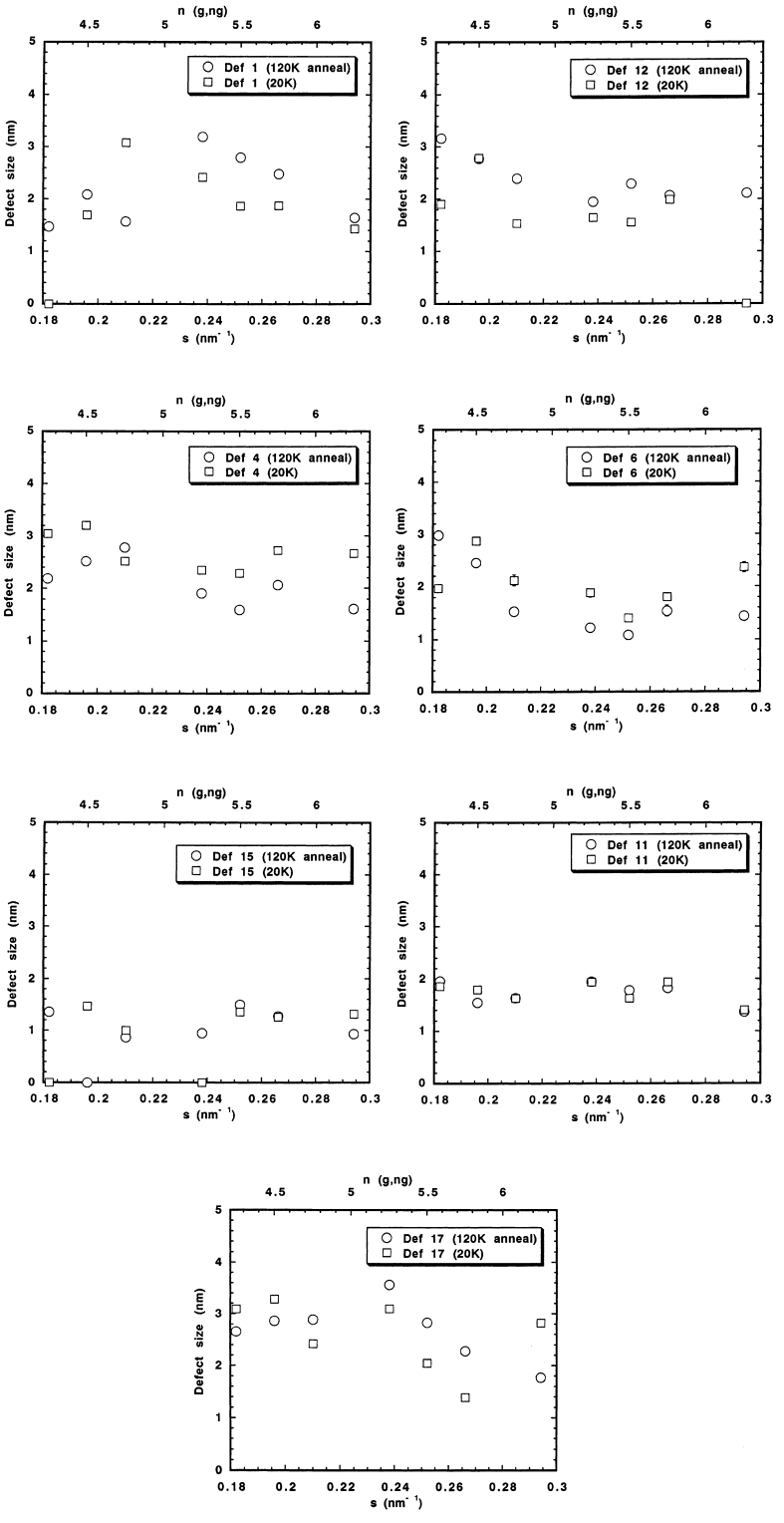

Fig. 4. Size measurements as a function of deviation parameter, *s*, for the defects labeled in Fig. 3 and discussed in the text.

arrow is the distance of the projected ion track through the foil thickness (55 nm). This results from a foil tilt of about 23° from the irradiation direction and coincident foil normal (near the 1 1 1 pole). Several clusters of defects can be seen in the 20 K labeled images to lie approximately along the irradiation direction and over distances equal to the arrow length.

Several features are apparent. The pair of micrographs taken before the anneal show the small contrast differences expected when s is varied – individual defects show variations in contrast intensity and apparent size, and a few are visible in one micrograph but not the other – but generally they look similar. The same is true of the pair of micrographs taken after the anneal. However, comparison of micrographs taken at the same value of s before and after the anneal show more profound changes. This was confirmed by viewing the whole series of seven micrographs at different s values before and after the anneal.

Some defects of interest are arrowed and labeled. Examples of defects which disappear upon anneal are labeled *d*. Those which appear upon anneal are labeled *a*. Examples of defects which shrink in size are labeled 4 and 6, those which grow are labeled 1 and 12. Defects which stay the same size are labeled 11 and 15, and one which shows inconsistent behavior (over seven s values) is labeled 17. The direction of the arrows of numbered defects corresponds to the direction of the size measurement.

Fig. 4 shows the quantitative measurements of image size for the above defect examples. Error bars on the size measurements are illustrated only for defect six, and are seen to be of the same size or smaller than the data point symbol. Defects were determined to have grown or shrunk in size only if six of seven s values showed consistent directions of the size change.

Within a field of view somewhat larger than that illustrated in Fig. 3, a total of about 150 defects were imaged before the anneal to 120 K. Of these defects, about 100 remained after the anneal and we measured the sizes before and after annealing of 55 of them. A comparable number of defects, 44 disappeared and 55 appeared upon anneal. Of the 55 defects measured for a size change, three grew and seven shrunk, using the consistency criteria. The large majority (45) of the measured defects showed no consistent change in size exceeding our measurement sensitivity of about 0.5 nm. In other cases, groups of closely spaced defects persisted through the anneal, but with apparent changes in morphology, and these were not analyzed.

In the video experiment, some defects were also seen to disappear and appear. The contrast of those clusters which disappeared faded over a period of tens of seconds or longer at temperatures between about 30 and 80 K. New clusters also appeared gradually over the same temperature range, sometimes in the same or similar positions as clusters which had earlier disappeared. There was no evidence for defect motion. A very small slow change in diffraction condition during the course of the anneal was detected in the image background and may explain at least some of the defects gradually disappearing or appearing, certainly those which reappeared in the same position.

Fig. 5 shows exactly the same area imaged at 20 K in $g = 002$ in the weak beam diffraction condition g, 5.5 g after approximately 15 min anneals to 120 and 300 K.

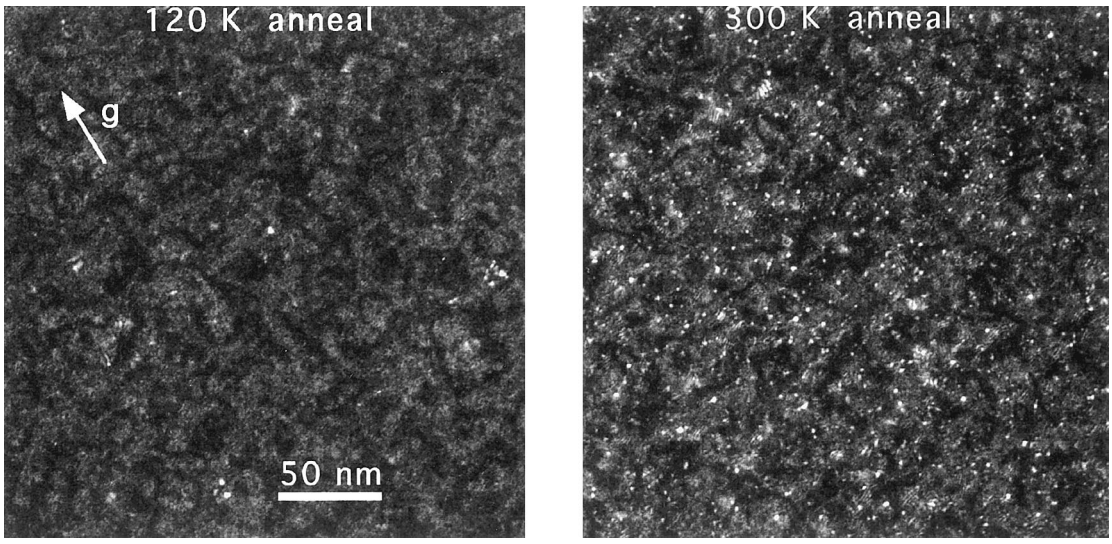

Fig. 5. TEM micrographs of the same area imaged at 20 K in $g = 002$ dark field in the weak beam condition g, 5.5 g after 15 min anneals to 120 and 300 K.

The appearance of a high density of small defects after the 300 K anneal occurred only in the area where the electron beam was incident for a significant time at 20 K. The density of these defects is so high that it is not possible to determine the fate of the clusters present in this area prior to the anneal to room temperature. Qualitatively, stereo images showed the new defects to be concentrated near the back surface of the foil. These defects range in size from 2 down to 0.5 nm, and some display contrast typical for stacking fault tetrahedra, implying a vacancy nature.

The low temperature dependence of cluster defect production can be rather closely compared in these experiments, as illustrated in Fig. 6. Areal defect density measurements were made on micrographs obtained after the irradiation at 20 K, and were compared with similar measurements made on specimens irradiated at room temperature with Cu^+ ions of the same energy and dose (see Ref. [10]). When allowance was made for the difference in foil thickness, the volume densities were equal within experimental error. However, there was a substantial difference in defect sizes, the lower irradiation temperature produced the smaller cluster defect sizes. The defects formed at 20 K showed no evidence of SFT formation. Of the defects formed at 300 K, less than 10% showed evidence for SFT formation. In a foil of thickness 60 nm, each incident 600 kV Cu^+ ion produced on average three visible clusters.

4. Discussion

We consider first the measurements on the size changes of defects annealed to 120 K (Fig. 4). A large majority of defects showed no measurable change in size, corresponding to a size change of less than about 0.5 nm. Of those defects whose measured size changes exceeded statistical error, the majority showed size decreases. This evidence of shrinkage implies that these loops are probably vacancy in nature. Vacancy loops would be expected to shrink by the absorption of freely migrating interstitials in Stage I. However, a small minority showed size increases and are judged, therefore, on the same argument, to be interstitial in nature. Since only a small number of defects show this behavior this result must be regarded as tentative.

In contrast to the limited result on the size measurements on the defects which persisted through the 120 K anneal, was the interesting and unexpected result that a comparable number of defects either disappeared

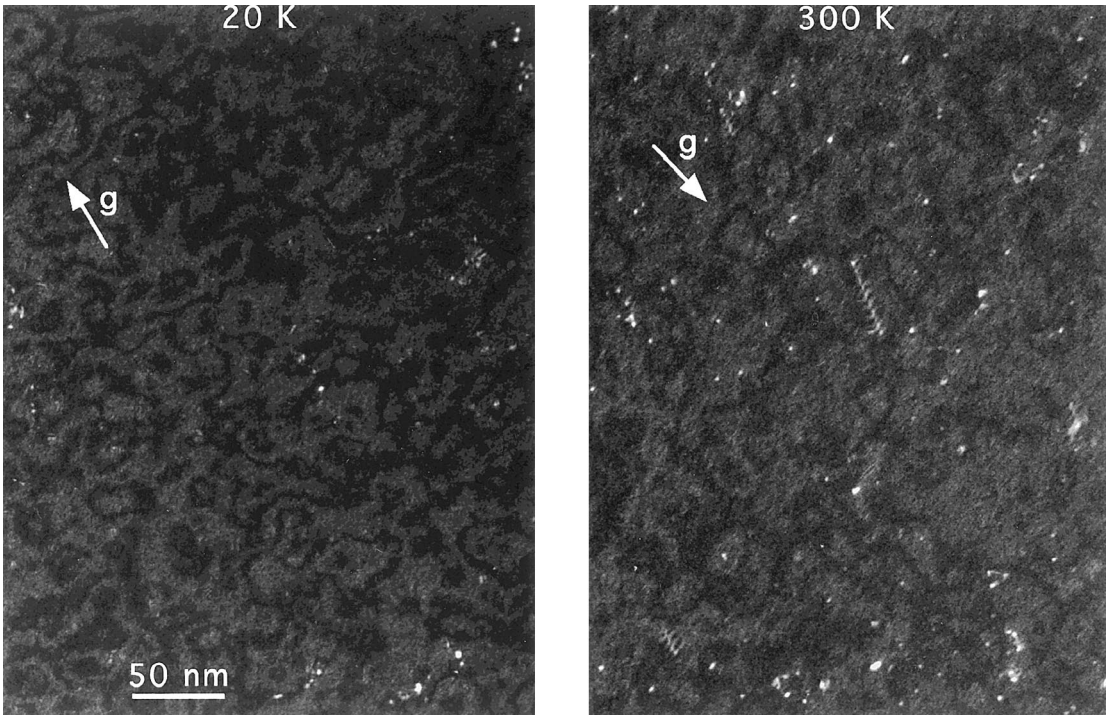

Fig. 6. TEM micrographs comparing irradiation temperatures of 20 and 300 K. Imaging conditions for both were $g = 002$ dark field and weak beam condition g, 5.5 g. Cu foil thicknesses were measured by convergent beam technique to be 55 nm for the exact area in the left panel and 65 nm for the exact area in the right panel. The irradiation in both cases was 600 keV Cu ions to a dose of 5×10^{14} m^{-2}.

or appeared upon the anneal. It is to be emphasized that these changes were certainly brought about by the anneal. At 20 K, defects were stable under the electron beam for extended periods. Re-annealing specimens which had been annealed to 120 K and then cooled to 20 K did not result in similar effects.

Possible mechanisms for the appearance of new loops include thermally induced collapse of vacancy-rich depleted zones (seen previously by Vetrano et al. [12]) and interstitial clustering. Disappearance could be caused by complete recombination of vacancy loops by freely migrating interstitials. Alternatively, the observation could be due to the movement of glissile loops along their glide cylinders from one position to another.

The video evidence seems to rule out this last possibility. Defects were never seen to move from one position to another, or to slip out of the foil. However, other aspects of the interpretation of the video experiment are complicated by possible artifacts. Since the resolution of the video system is limited, the smallest defects may not be resolved. As the specimen warmed up from 20 to 120 K, a small amount of specimen bending occurred, and so the diffraction conditions changed. Since the contrast of small clusters is known to be very sensitive to s, the apparent disappearance and appearance of defects in the video experiment may be a contrast artifact. This may explain why defects sometimes 'appeared' in the same positions as defects had earlier 'disappeared'. However, since images were over a complete range of s values in the main experiment, the possibility that the whole observation is an imaging artifact can be discounted.

At present we are unable to make a definitive judgement on the nature of the defects which disappear and appear. The gradual appearance or disappearance at temperatures when interstitials and interstitial clusters become mobile may favor interstitial clustering and shrinkage of vacancy loops. The fact that only some defects shrink may be explained by a very inhomogeneous free interstitial concentration which would be expected for this type of low dose ion irradiation. There was no obvious difference in morphology between defects which disappeared and those which persisted through the anneal.

The high density of small stacking-fault tetrahedra which appeared on warming specimens to room temperature is most likely due to the clustering of vacancies produced by surface sputtering due to the electron beam. Evidence for this is that these SFT appeared close to the electron-exit surface of the foil only in regions that had been exposed to the electron beam at low temperatures. As expected, the effect was more pronounced at higher beam energies, which would be expected to increase the sputtering rate. At the low temperature vacancies produced by surface sputtering are immobile, and a high concentration can build up close to the bottom surface of the foil. On warming through Stage III these cluster into the observed SFT. This process undoubtedly occurs under electron irradiation at 300 K and 100 keV, except that the instantaneous concentration of vacancies is always too low to produce cluster defects of significant or visible size. In copper, the maximum recoil energy at 100 keV electron energy is 3.8 eV. If the known sublimation energy of 3.5 eV can be related to a sputtering threshold energy, then an electron beam energy of 80 keV, with a maximum recoil energy of 3.0 eV, should be sufficient to eliminate this effect in copper.

In comparing the visible defect yield between irradiation temperatures of 20 and 300 K, it was quite interesting to find that the mechanism for collapsing the defect cascade into a cluster defect, such as a dislocation loop, appears equally effective at the two temperatures. It is, however, more efficient at 300 K in clustering a higher fraction of produced vacancies (or interstitials), based on the larger defect sizes. This independence of cluster defect density on irradiation temperature from 20 to 300 K, agrees with similar measurements made on Cu by Daulton et al. [13], but is in striking disagreement with measurements made on Ni [14].

A comparison with collision statistics calculated by TRIM is particularly instructive. For a single 600 keV Cu ion passing through a Cu foil of 60 nm thickness, TRIM finds (averaged over 10 000 ions) three recoils with energy >6 keV. Since the experiment finds three defects per ion, this implies that collision cascades produce visible cluster defects down to the surprisingly low recoil energy of 6 keV, and with a probability (yield) of one. All previous experimental values of defect yield per ion at low incident energies (30–50 keV) and thus near surface (10–15 nm), such as Fukushima et al. [7], fall in the range 0.4–0.5. This suggests that in these earlier experiments, the presence of a surface lowers the probability of cluster defect production, possibly through loss of individual or cluster defects to the surface.

5. Conclusions

A low temperature in situ ion-irradiation and annealing experiment has been performed in copper. Copper foils were irradiated with 600 kV Cu^+ ions at 20 K in the low temperature stage of the Argonne Hitachi-9000 electron microscope. A modified weak-beam technique was used to investigate the changes in size of defect clusters which remained identifiable on annealing to 120 K. Most clusters showed no size changes within the resolution of the sizing technique (0.5 nm). A small fraction of about 10% of these showed measurable size decreases, while a very small number showed size increases. We argue that these clusters are likely to be of vacancy and interstitial nature, respectively.

Also on annealing to 120 K a fraction of about 25% of the clusters disappeared entirely, while a similar number of clusters appeared at different locations. The remaining defects persisted through the anneal, sometimes however with modified morphologies. Video microscopy suggested that the disappearance and appearance of clusters occurred gradually and was unlikely to be due to loop movement. Clusters appeared or disappeared over a period of tens of seconds or minutes at temperatures in the range 30–80 K. At present we are unsure of the likely nature of these clusters.

On warming specimens to room temperature a high density of small SFT appeared close to the electron-exit surface of the foil in regions which had been exposed to the electron beam at low temperatures. These are most likely due to the clustering of vacancies produced by surface sputtering.

Acknowledgements

This work was supported by the US Department of Energy, BES-Materials Science, under DOE contract # W-31-109-Eng-38. We thank E.A. Ryan, L. Funk, A. McCormick of the Argonne Accelerator-IVEM User Facility for technical assistance, B. Kestel and T.L. Daulton of ANL for help in preparing specimens, and S. Ockers of ANL and A.K. McKnight of Oxford for photographic assistance.

References

[1] T.D. de la Rubia, M.W. Guinan, Phys. Rev. Lett. 66 (1991) 2766.
[2] A.J.E. Foreman, W.J. Phythian, C.A. English, Philos. Mag. A 66 (1992) 671.
[3] D.J. Bacon, A.F. Calder, F. Gao, V.G. Kapinos, S.J. Wooding, Nucl. Instrum. and Meth. B 102 (1995) 51.
[4] H. Fukushima, Y. Shimomura, M.W. Guinan, J. Nucl. Mater. 155–157 (1988) 1205.
[5] M.O. Ruault, H. Bernas, J. Chaumont, Philos. Mag. A 39 (1979) 757.
[6] H. Fukushima, M.L. Jenkins, M.A. Kirk, Philos. Mag. A 75 (1997) 1567.
[7] H. Fukushima, M.L. Jenkins, M.A. Kirk, Philos. Mag. A 75 (1997) 1583.
[8] M.C. Frischherz, M.A. Kirk, J.P. Zhang, H.W. Weber, Philos. Mag. A 67 (1993) 1347.
[9] J.F. Ziegler, J.P. Biersack, U. Littmark, The Stopping and Range of Ions in Solids, Pergamon, NewYork, 1985.
[10] M.L. Jenkins, M.A. Kirk, H. Fukushima, J. Electron Microsc. (1999) accepted.
[11] P.M. Kelly, A. Jostons, R.G. Blake, J.G. Napier, Phys. Stat. Sol. A 31 (1975) 771.
[12] J.S. Vetrano, I.M. Robertson, M.A. Kirk, Scripta Met. 24 (1990) 157.
[13] T.L. Daulton, M.A. Kirk, L.E. Rehn, these Proceedings, p. 258.
[14] I.M. Robertson, J.S. Vetrano, M.A. Kirk, M.L. Jenkins, Philos. Mag. A 63 (1991) 299.